LBL-31526

Lawrence Berkeley Laboratory
UNIVERSITY OF CALIFORNIA

Accelerator & Fusion
Research Division



Presented at the Accelerator Instrumentation Workshop,
Newport News, VA, October 28–31, 1991,
and to be published in the Proceedings

# Advanced Light Source Beam Position Monitor

J. Hinkson

October 1991

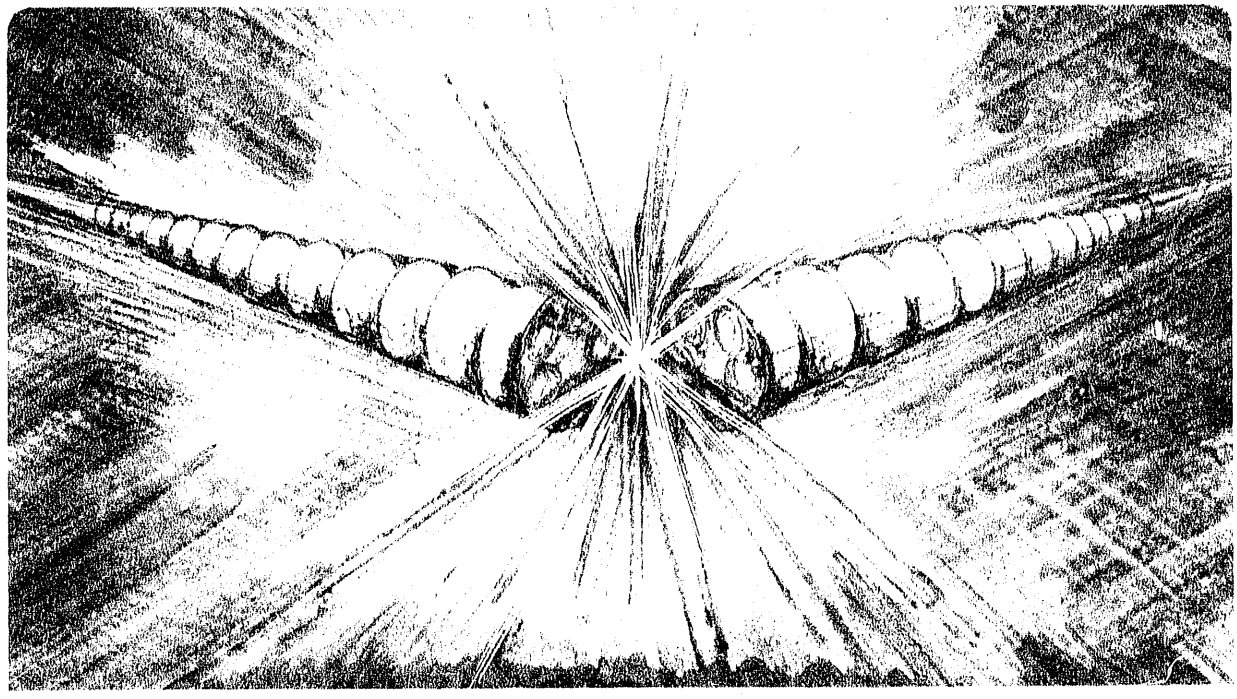

Prepared for the U.S. Department of Energy under Contract Number DE-AC03-76SF00098

LBL--31526

DE92 010268

# ADVANCED LIGHT SOURCE BEAM POSITION MONITOR*

Jim Hinkson

Advanced Light Source
Accelerator and Fusion Research Division
Lawrence Berkeley Laboratory
University of California
Berkeley, CA 94720

October 28, 1991

Paper Presented at the Accelerator Instrumentation Workshop, CEBAF, Newport News, VA, October 28–31, 1991



*This work was supported by the Director, Office of Energy Research, Office of Basic Energy Sciences, Materials Sciences Division of the U.S. Department of Energy, under Contract No. DE-AC03-76SF00098

# Advanced Light Source Beam Position Monitor

J. Hinkson
Lawrence Berkeley Laboratory, Berkeley CA 94720

## Abstract

The Advanced Light Source (ALS) is a synchrotron radiation facility nearing completion at LBL. As a third-generation machine, the ALS is designed to produce intense light from bend magnets, wigglers, and undulators (insertion devices). The facility will include a 50 MeV electron linear accelerator, a 1.5 GeV booster synchrotron, beam transport lines, a 1-2 GeV storage ring, insertion devices, and photon beam lines. Currently, the beam injection systems are being commissioned, and the storage ring is being installed. Electron beam position monitors (BPM) are installed throughout the accelerator and constitute the major part of accelerator beam diagnostics. The design of the BPM instruments is complete, and 50 units have been constructed for use in the injector systems. We are currently fabricating 100 additional instruments for the storage ring. In this paper I discuss engineering, fabrication, testing and performance of the beam pickup electrodes and the BPM electronics.

## Introduction

The beam position monitors for the ALS have been discussed before in a brief paper[1]. In the space allowed here I report on the engineering problems and solutions in greater detail. Each BPM system is composed of an array of beam pickup electrodes, a set of high-quality coaxial cables, a bin of processing electronics, and a controlling computer. These components will be fully treated in the following pages.

The storage ring circumference is 200 meters. It has 12 curved sections each about 10 meters long and 12 straight sections of 6.7 meter length. Two of the straight sections are used for beam injection and RF cavities. The remaining straight sections are reserved for insertion devices. BPMs are installed in the curved sections only (96 total, 8 per section). The booster synchrotron circumference is 75 meters and is composed of four curved and four straight sections. Thirty-two BPMs are installed nearly uniformly around the ring. Table I shows accelerator parameters relevant to beam diagnostics.

**Table I. Accelerator Parameters for Beam Diagnostics**

| Parameter | Storage Ring | Booster | Linac |
|---|---|---|---|
| Energy (GeV) | 1-2 | 0.05-1 | 0.05 |
| RF Frequency (MHz) | 499.654 | 499.654 | 2998 |
| Harmonic Number | 328 | 125 | - |
| Minimum Bunch Spacing (ns) | 2 | 8 | 8 |
| Revolution Period (ns) | 656 | 250 | - |
| Number of Bunches | 1-250 | 1-12 | 1-20 |
| Repetition Rate (Hz) | - | 1 | 1-10 |
| Maximum Average Current (mA) | 400 | 20 | 125 |
| Single Bunch Current (mA) | 8 | 3 | 10 |
| Bunch Length ($2\sigma$ ps) | 28-50 | 100 | 30 |
| Tune $\nu_h, \nu_y$ | 14.28, 8.18 | 6.26, 2.79 | - |
| Synchrotron Frequency $f_s$ (kHz) | 13.87 | 256-44 | - |

## Requirements

The storage ring BPMs are required to make continuous, non-destructive measurements of average beam position during beam injection and stored beam lifetime. Fully corrected beam position data will be delivered to the beam orbit control computer at 10 Hz. In addition, single-turn position data is to be accumulated at the ring revolution frequency and stored in internal BPM memory.

The booster ring BPMs function similarly to those in the storage ring with the performance specifications being less rigorous. Average beam position at a selected time in the booster energy ramp (0-0.4s) is reported at 1Hz. Single turn measurements are made also. The booster ring revolution frequency is higher, 4MHz, making single turn measurement timing a little more difficult.

BPMs in the Linac and beam transport lines measure beam at 1 to 10 Hz. There are 17 BPMs located in these areas. The beam repetition rate is low here, so we have slightly modified the storage ring BPM design to accommodate this lower rate. Table II shows the basic specifications for the BPMs in the different accelerator areas.

**Table II. BPM Performance Specifications**

| Parameter | Storage Ring | Booster | Linac |
|---|---|---|---|
| Resolution (low speed) (mm) | 0.01 | 0.1 | 0.1 |
| Resolution (high speed) (mm) | 0.5 | 0.5 | - |
| Repeatability (low speed) (mm) | 0.03 | 0.1 | 0.5 |
| Repeatability (high speed) (mm) | 0.5 | 1.0 | - |
| Data Storage (turns) | 1023 | 1023 | - |
| Low Speed Response (Hz) | 20 | 1 | 1 |
| High Speed Response (MHz) | 5 | 7 | - |
| Dynamic Range (dB) | 40 | 40 | 50 |
| Center Frequency (MHz) | 500 | 500 | 500 |
| Beam Pickup Style | Button | Button | Button and Stripline |
| Pickup Coupling (ohm @ 500MHz) | 0.1 | 1.0 | 1.0 and 8.0 |

## Measurement Method

Shafer[2] and Littauer[3] have reported on the various methods used to determine transverse position of a charged particle beam. At the ALS we use the difference-over-sum technique which is most often used in synchrotron light sources. Our beam pickups consist of two pairs of electrodes mounted in the beam vacuum chamber wall. Beam signals induced in these electrodes travel via coaxial vacuum feedthroughs and coaxial cables to the BPM electronics where the signals are processed to reveal the X and Y position of beam center of charge. At nearly all locations in the ALS beam is composed of short electron bunches, between 10 mm and 30 mm, FLHM (Full Length Half Maximum). A 10 mm relativistic bunch corresponds to a pulse duration of about 33 ps FWHM (Full Width Half Maximum). In the booster and storage rings these short bunches are periodic and contain harmonics of equal amplitude extending into the multi-GHz region. Position information is contained in the amplitude of any of the harmonics sensed by the electrodes. By amplifying and detecting the amplitude of a selected harmonic we determine beam position by taking the difference between detected signals from two opposed electrodes, dividing the result by their sum, and multiplying that result by the reciprocal of a sensitivity constant. For example, beam position as measured by two horizontally opposed pickup electrodes would be calculated as follows:

$$X = \frac{V_1 - V_2}{V_1 + V_2} \frac{1}{S_x} \qquad (1)$$

where V1 and V2 are amplitudes of detected beam harmonics and Sx is a constant in % / mm.

**Storage Ring Beam Pickup Electrodes**

We use button style electrodes for BPM pickups in the storage ring. The major reason for using them instead of other pickup devices is because of their low beam impedance. Coupled bunch beam instabilities (a major problem in storage rings with many short bunches and high average current) are driven by energy stored in reactive impedances in the vacuum chamber. With nearly 400 BPM pickups in the storage ring, we were concerned about their impact on a rather limited narrow-band beam impedance budget. Another reason for using buttons is that they may be precisely fabricated and installed with good accuracy.

A button pickup is usually a thin, circular metal disk supported by the center conductor of a coaxial vacuum feedthrough. The button is mounted flush with the wall of the beam vacuum chamber to avoid being struck by the beam. Where synchrotron radiation is present the buttons are configured to avoid being struck by the radiation, or a mask is installed to intercept the radiation. At least four buttons are used in a combined function monitor to determine horizontal and vertical beam position. Since the beam bunch length in electron rings is usually very short, it is common to make the button diameter equal to twice the rms beam bunch length ($2\sigma$) in order to collect maximum charge and to have good position sensitivity. Generally, peak current in the beam bunch is high, so signal strength for the BPM electronics is not a problem. A fraction of the beam bunch charge appears as voltage on the button self-capacitance to ground. Usually the capacitance is loaded by 50 Ω, resulting in a high-pass configuration for the beam signal.

Excellent button and coaxial feedthrough devices suitable for ultra-high vacuum service are available from industry today. The feedthroughs typically have well controlled impedance and are free of resonances up to 10 GHz or higher. Feedthrough and button installation in the vacuum pipe is accomplished by either welding the feedthrough into a flange which is later attached to the beam pipe or by welding the feedthrough into a section of the vacuum pipe directly. In both of these cases the exact location of the button face relative to the geometric center of the beam pipe is difficult to determine. Mechanical and electrical offsets in the button array are found by wire antenna measurements when practical or by external measurements. In the ALS storage ring we chose not to use either of these button installation methods. There were two reasons for this. Our unusual vacuum chamber prevented us from fabricating and characterizing a pickup assembly which we could later attach to the chamber. Secondly, we were very concerned with the mechanical precision and stability of the button installation. We felt that a button welded in place would not meet our accuracy requirements.

The ALS storage ring vacuum chamber is not the usual stainless-steel pipe or extruded aluminum chamber most often used in storage rings. The 10-meter curved vacuum chambers are formed by two machined pieces of aluminum which are welded together. Large slabs of aluminum (10.3 x 1.5 x 0.1 meters) were machined by a numerically-controlled, 5-axis mill. Very intricate machining was performed on the top and bottom of the slabs to accommodate magnet pole tips, flanges, diagnostic ports, BPM pickups, photon stops, vacuum pumps, and the electron beam channel. The beam chamber is somewhat diamond shaped and is open to an anti-chamber on the outer radius. The anti-chamber is used for vacuum pumping, photon stops, and photon ports.

Having a machined chamber with thick walls afforded us the opportunity to place holes for the BPM pickup electrodes (buttons) with good accuracy relative to survey points on the chamber itself. Our intent was to position the electrodes precisely in the chamber holes using a machined ceramic spacer and to hold the electrodes in place with a spring-loaded coaxial vacuum feedthrough. In this case neither feedthrough welding or flange placement determined the location of the pickup electrode. RF contact between pickup components was made with "Multilam" RF fingers. The fingers provided enough mechanical compliance to remove transverse stress from the vacuum feedthrough. Figure 1 shows the installation scheme for the pickup and related parts.

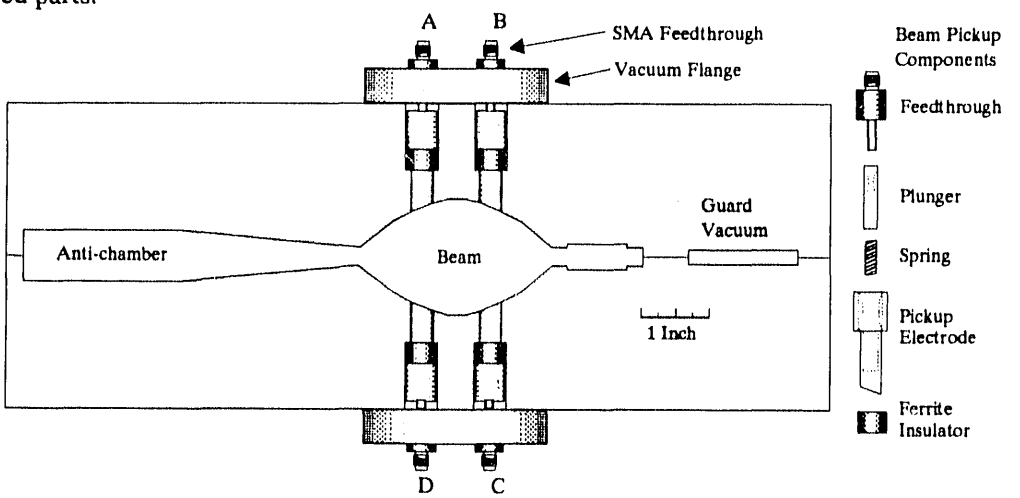


Fig. 1 Cross section of ALS storage ring BPM buttons with exploded view of button parts. Shaded area is a very simplified representation of vacuum chamber.

Figure 1 illustrates the pickups installed vertically with two feedthroughs welded into a single vacuum flange. Notice the pickup face exposed to the beam is beveled to conform to the vacuum chamber wall. This was not our original design. In the prototype full sized vacuum chamber the BPM pickup holes were drilled at 25 degrees off vertical making the flat-faced electrodes fit flush to the beam chamber wall. The prototype chamber construction program revealed that the milling machine could not hold our machining tolerances at a 25 degree angle, so the holes were drilled vertically in the 12 production chambers. This made it necessary for us to bevel the pickup face and install a ceramic key to prevent pickup rotation.

While our BPM pickup design may have had certain mechanical virtues, we faced a number of electrical problems. The pickup is essentially a loss-less capacitor at low frequencies, but in the microwave region it exhibits annoying resonances. These resonances are due to the different radii of the pickup components. The pickup is composed of five short transmission lines of differing characteristic impedance. The end transmission line (the pickup electrode) is open-ended. These transmission lines are resonators at microwave frequencies all of which can be excited by the short beam bunch. We detect these resonances by network analyzer measurements of either S11 at the SMA connector or S21 from the beam side of the pickup. The shunt impedance of these narrow band resonances (5 GHz and up) exceeded our impedance budget. We damped the Q of these resonances by replacing the ceramic spacer and anti-rotation key with NZ31 lossy ferrite. This brought the total narrow-band impedance of all the pickups back within limits and increased the low frequency pickup capacitance to about 25 pF.

Another problem appeared when we placed two feedthroughs on a single flange. The coupling between adjacent buttons rose from a figure of about -100 dB (with feedthroughs on separate flanges) to about -40 dB. There was sufficient space in the tiny gap between the flange and vacuum chamber (due to the metal vacuum seal) for coupling between the feedthrough center-conductors at 500MHz. To determine button electrical center offset due to electrical and mechanical imperfections, we required that coupling between the pickups be between the button faces only. We eliminated the feedthrough coupling by installing RF seals around each center conductor at the flange-to-chamber interface. In spite of the difficulties we have experienced with the storage ring buttons, we feel we have an adequate design. They are accurately placed in the vacuum chamber, and tooling ball fixtures near the buttons allow us to measure their position relative to upstream quadrupole magnet survey points.

**Storage Ring Pickup Testing**

A small prototype vacuum chamber was fabricated in two halves and fitted with our button pickups. The chamber was placed in a test set that allowed us to install a movable wire to simulate beam and to close the ends of the chamber. Actually, the wire is stationary, and the chamber is moved. Closing the camber ends prevents spurious operation but makes wire installation difficult. Having the chamber in two halves solves that problem. The wire, #30 gauge, is terminated in its characteristic impedance, 290 ohms, to minimize standing waves in the chamber. Part of the 290 ohms is the 50 ohm load on the network analyzer reference (R) port. See figure 2. The wire is driven by the RF output of a HP8753 network analyzer. We move the chamber using a precision X-Y stage and measure the response of the buttons. This is done to determine the sensitivity of the buttons to beam motion, find the beam coupling impedance, and determine the extent of button nonlinear coupling at large beam (wire) displacements. Small sight holes drilled in the X and Y planes near the pickups permit us to position the wire to within 0.01 mm of mechanical center.

It is apparent in Fig. 2 that a large impedance mismatch occurs at the entrance of the test chamber. The source impedance of the network analyzer absorbs reflected voltages. Normalizing the measured button signals to the analyzer R port reduces the effects of the impedance mismatch and the changing Zo of the wire as it is moved far off center. We determined that the storage ring button sensitivity is:

$$S_x = 7.67\%/\text{mm}$$
$$S_y = 5.72\%/\text{mm}$$

The linear equations used to determine beam position are:

$$X = \frac{(V_a + V_d) - (V_b + V_c)}{(V_a + V_b + V_c + V_d)} \frac{1}{S_x} \qquad (2)$$

$$Y = \frac{(V_a + V_b) - (V_c + V_d)}{(V_a + V_b + V_c + V_d)} \frac{1}{S_y} \qquad (3)$$

where Va, Vb, Vc, and Vd are detected button signals (see figure 1).

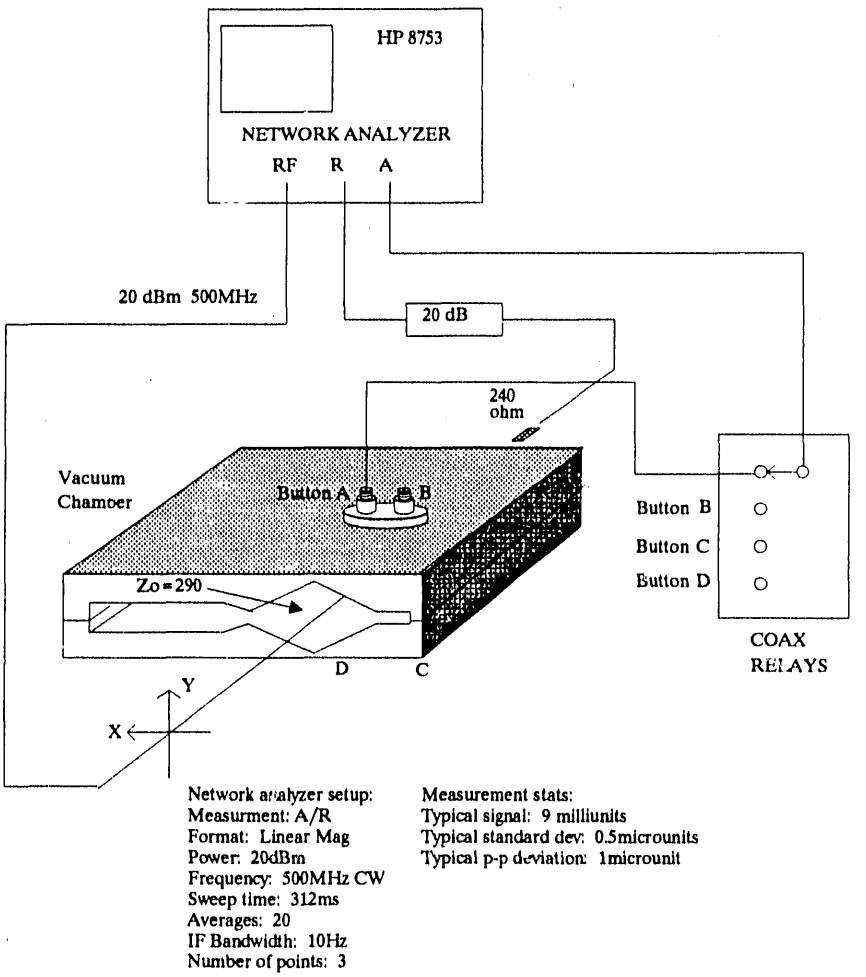


Fig. 2 Diagram of storage ring BPM button test set. The 290 ohm wire is moved in X and Y as the button response is measured by the net' ork analyzer.

Since the buttons are not placed in the measurement axes, we must use all four signals to calculate either X or Y beam position. Equations (2) and (3) are valid (for the 0.03 mm accuracy specification) for deflections less than 2 mm off center. In order to make accurate position measurements at larger displacements and correct for pin-cushion nonlinearities we make use of the method developed by Halbach[4]. In this development the response of the four buttons is determined for any beam position X,Y,

$$V_i = f_i(X,Y) \qquad (4)$$

where $f_i(X,Y)$ is a Taylor series whose coefficients are uniquely determined for the vacuum chamber cross-section and button locations using POISSON, an electrostatic analysis program. Then the two coupled equations

$$g(X,Y) = \frac{(V_a + V_d) - (V_b + V_c)}{(V_a + V_b + V_c + V_d)} \quad (5)$$

$$h(X,Y) = \frac{(V_a + V_b) - (V_c + V_d)}{(V_a + V_b + V_c + V_d)} \quad (6)$$

are solved numerically for X and Y using a fast converging iterative program resident in the local computer. For our storage ring eight Taylor series coefficients are used. We tested the validity of this approach by taking data from many wire locations as far as 20 mm off center. At 20 mm displacement the calculation had 0.1 mm error. The linear position calculation at 20 mm was off by more than 5 mm.

Additional testing of the storage ring buttons was required. While the buttons may be accurately positioned, significant errors occur due to electrical offsets. The contributors to these errors are unequal button capacitance, connector insertion loss, and coaxial cable attenuation. The button capacitance is nominally 25 pF. We measure 10% capacitance variations between buttons. These variations cause a noticeable offset of electrical zero in a four-button array. There are minor differences in the SMA connector insertion loss. The cables we attach to the buttons are nominally 100 feet long. Their attenuation at 500 MHz is not exactly equal. The effect of all of these offsets is compensated by a measurement of the button-to-button transfer function at our operating frequency, 500 MHz. This measurement is performed twice, once when the buttons are installed in the chamber as a quality assurance step, and again when the cables have been attached. This technique[5] compensates unlike gain in the four channels and some degree of mechanical error. We have determined that mechanical offsets of up to 1mm in a button may be compensated with this technique. Tests on BPM buttons at the Argonne Advanced Photon Source[6] have shown good agreement between offsets measured with a wire and the button-to-button transfer function measurement. Performing these measurements when the buttons and cables are first installed has the additional benefit of providing us a data base of information against which we can compare future measurements. Fig. 3 is shows the setup we use to measure the transfer function between buttons in storage ring BPMs.

**Booster BPM Pickups**

The booster synchrotron is 75 meters in circumference and is composed of 4 arcs and 4 straight sections. Each arc has 7 BPM pickup arrays and each straight has a single array. Each array is composed of four button style pickups rotated 45 degrees from the horizontal plane. Figure 4 shows the button layout. We fabricated our own button assemblies using MDC type N constant impedance vacuum feedthroughs. Each button has about 25 pF low-frequency capacitance. Up to 3 GHz the buttton assemblies exhibit no resonances. Resonances do occur at higher frequencies but are of no concern because the impedance budget for the booster is more liberal than that for the storage ring. The booster BPM system is not required to perform as accurately as the storage ring system, so minor offsets are not important. However, we have tested the booster buttons and cables using the transfer function method anyway to gather baseline performance data.

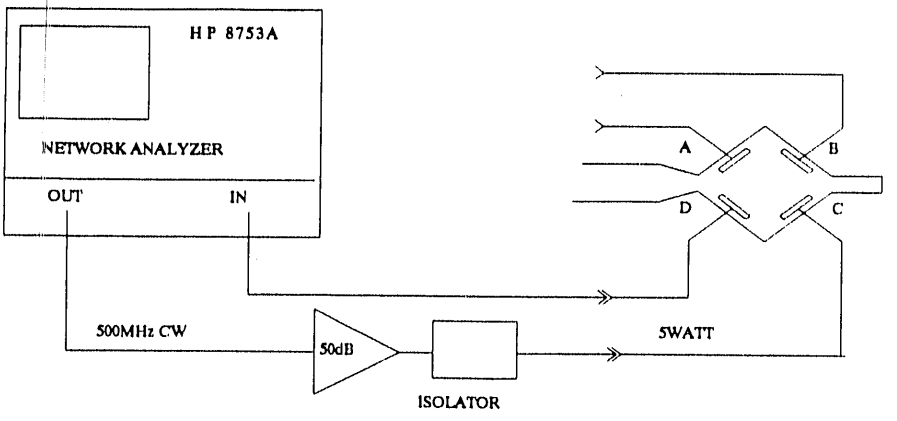


TYPICAL DATA
(numbers are in dB below a "Thru" reference)

| | |
|---|---|
| A to B -103.4 | C to D -104.17 |
| B to A -103.29 | D to C -104.16 |
| A to C -107.55 | B to D -107.47 |
| C to A -107.58 | D to B -107.50 |
| A to D -96.156 | B to C -95.630 |
| D to A -96.174 | C to B -95.632 |

Fig. 3 Diagram of button-to-button transfer function measurement. The power amplifier is required to extend the dynamic range of the analyzer at high values of attenuation.

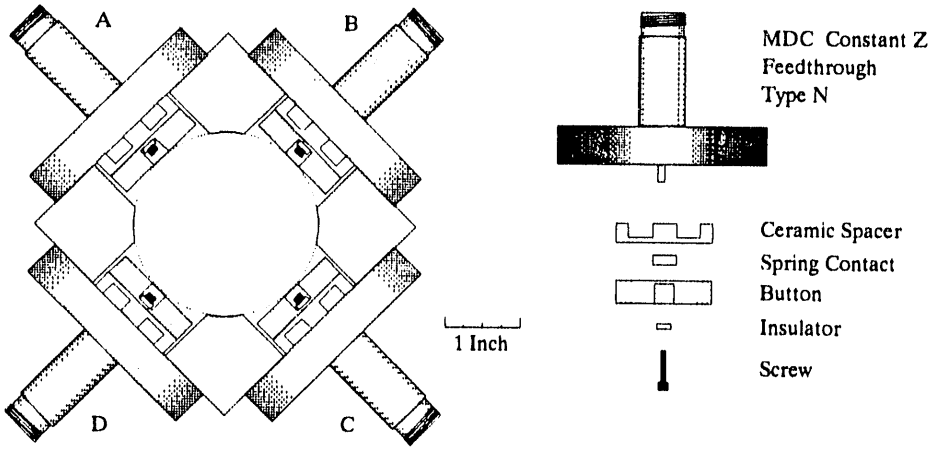


Fig. 4. Booster BPM button arrangement.

### Linac and Transfer Line BPM Pickups

Two types of beam pickups are used in these locations. In the Gun-to-Linac (GTL) section where longitudinal space is limited we installed the CERN LEP[7] button. This device is available from Ceramex (MetaCeram) in France. It was carefully engineered for broadband response. The

button itself is a thin disk about 1.25 inches in diameter. The disk is supported by a very good coaxial feedthrough that exhibits less that 0.05$\rho$ (reflection coefficient) up to 18 GHz. The button assembly has a 2.75 inche Conflat flange and is ready for installation upon delivery. The four-button arrangement is similar to the booster configuration except that the buttons are not rotated 45 degrees. We could have used the LEP buttons in the booster but we deemed it less expensive to construct our own. In retrospect the costs for either would probably have been about the same. Because of their excellent frequency response, we will use three sets of the LEP buttons as broadband beam monitors in the storage ring.

The remainder of the BPM pickups in the transfer lines are striplines. Fig. 5 shows the layout. These striplines are 150 mm long and have a $\lambda$ / 4 resonance at 500 MHz. This length was chosen to provide resonant drive for the 500 MHz bandpass filters in the detector electronics RF input section. All symmetrical striplines produce an inverted echo pulse (bunch length << stripline length) at a time 2l / c. With a length (l) of 150 mm, our stripline echo pulse occurs 1 ns after the prompt pulse providing resonant excitation for the filter.

The coaxial feedthroughs we used for the striplines are type N, constant impedance devices from Cermaseal. They have good performance to about 3 GHz. We observe ringing at 5 GHz in the stripline signal when it is excited by the short Linac beam pulse.

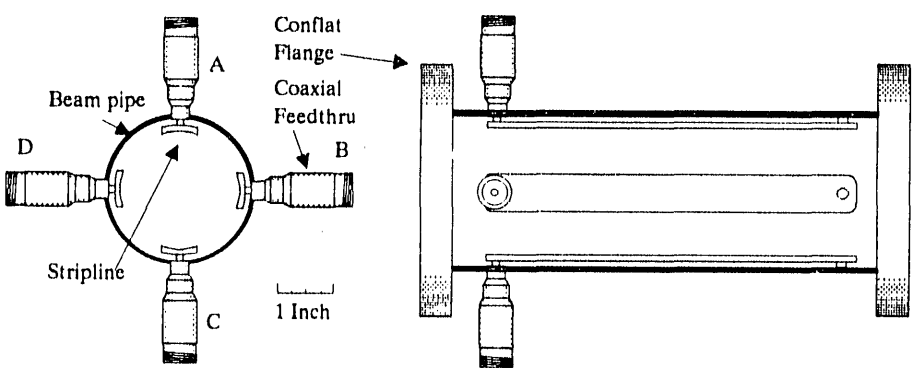


Fig. 5. Beam transfer line BPM striplines.

## BPM Electronics

A description of the storage ring BPM electronics follows. The BPMs for the booster and transfer lines are slightly different. As each BPM sub-system is described, the differences will be noted.

The BPM electronics are enclosed in Eurocard bins. The major sub-systems (except for the local oscillator, power supply, and programmable attenuator) are enclosed in 3U, plug-in modules fitted with metal enclosures. The module printed circuit boards are about 8.5 inches long and 4 inches high. The module enclosures are not RF tight. To help shield sensitive electronics we installed RF fingers on the top and bottom bin covers. When the module panel screws are tight and the covers in place, the instrument is relatively immune to RFI. All of the bin components and modules were supplied by Schroff. Figure 6 is a drawing of the bin and modules.

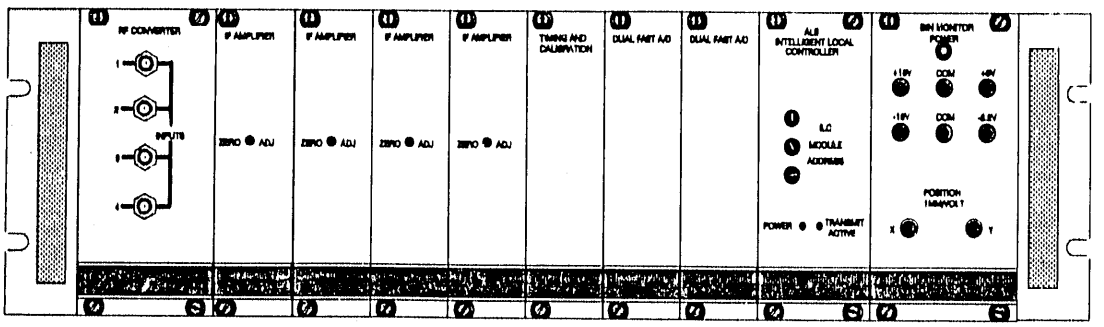

Fig. 6 Drawing of BPM modules and bin. The chassis is 19 x 5.25 inches.

The modules are electrically connected via 96-pin DIN connectors and a six-layer, full-width printed circuit board (back-plane). RF and video signals are routed between modules in coaxial cable and connected via coaxial inserts in special DIN 96-pin connectors. These connectors may have up to 8 coaxial feedthroughs. Nine of the conventional connector pins are lost for each coaxial connection. The coaxial cable connectors (from Palco) mate nicely with Belden 9307 cable, a small semi-rigid 50 ohm coax. Figure 7 shows the basic signal flow between modules.

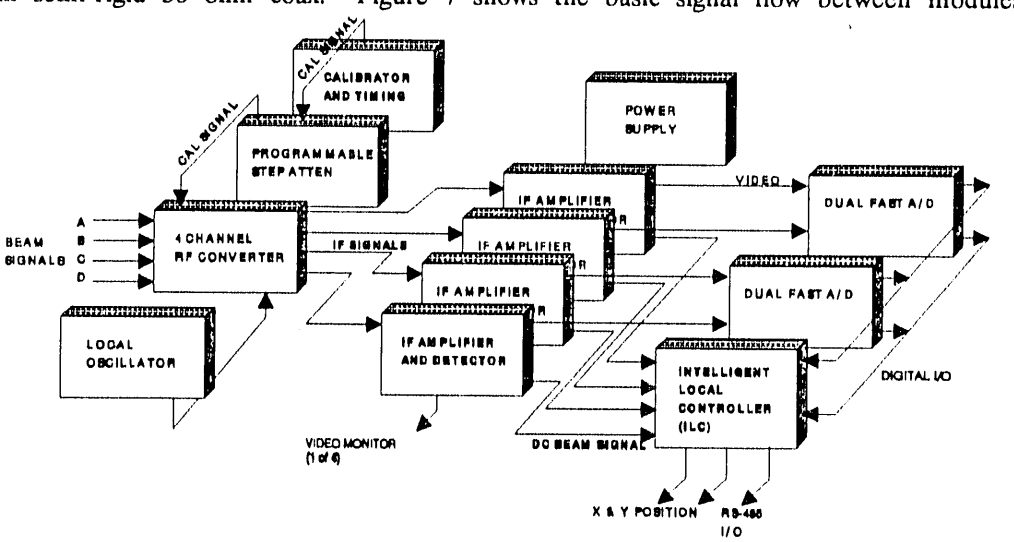


Fig. 7 Basic signal flow between BPM plug-in modules.

Throughout the ALS accelerator complex beam signals are routed to BPM electronics via Andrew FSJ1-50A Heliax cable. This cable was chosen because is has 100% shielding, polyethylene dielectric (more radiation tolerant than Teflon), good flexibility, and long-term stability. The cables terminate near the BPM electronic bins in N-to-SMA bulkhead feedthroughs. We will use .141 semi-rigid coaxial jumper cables to connect beam signals to the four-channel RF converter modules in storage ring BPMs. RG223 is used for the jumper cables in other locations. The connections are made on the front of the RF-modules via SMA connectors. While it would have been more convenient to make beam-signal connections through the BPM bin back panel and DIN connectors, we felt the front-panel SMA connections would be more reliable. All critical signal paths except the beam pickups, Heliax cables, and input connectors are in the BPM self-calibration loop. Therefore, components outside the loop must be stable and reliable.

Each BPM bin contains four super-heterodyne, amplitude-modulation receivers. Beam signals from four pickups are band-limited by the coaxial cables and bandpass filters and are down-converted to the 50 MHz intermediate frequency (IF) in the RF converter module. Four IF amplifier/detector modules process the RF converter output signals. The gain of the IF amplifiers is set by a single DAC output of the Intelligent Local Controller (ILC), the bin computer. The envelope of the IF signals is detected and sent in three paths. For error corrected measurements of average beam position the detector pulse output is peak-detected, filtered and digitized by the ILC. For single turn measurements of beam position the detector output pulse is again peak detected and digitized by a video ADC. The third path for the detector signal is to a monitor jack on the bin rear panel. Since the four IF amplifiers do not have equal gain an ILC controlled calibrator is available for test signal injection into the RF module. The block diagram in figure 8 illustrates the basic design. In the following sections each BPM module is discussed in detail.

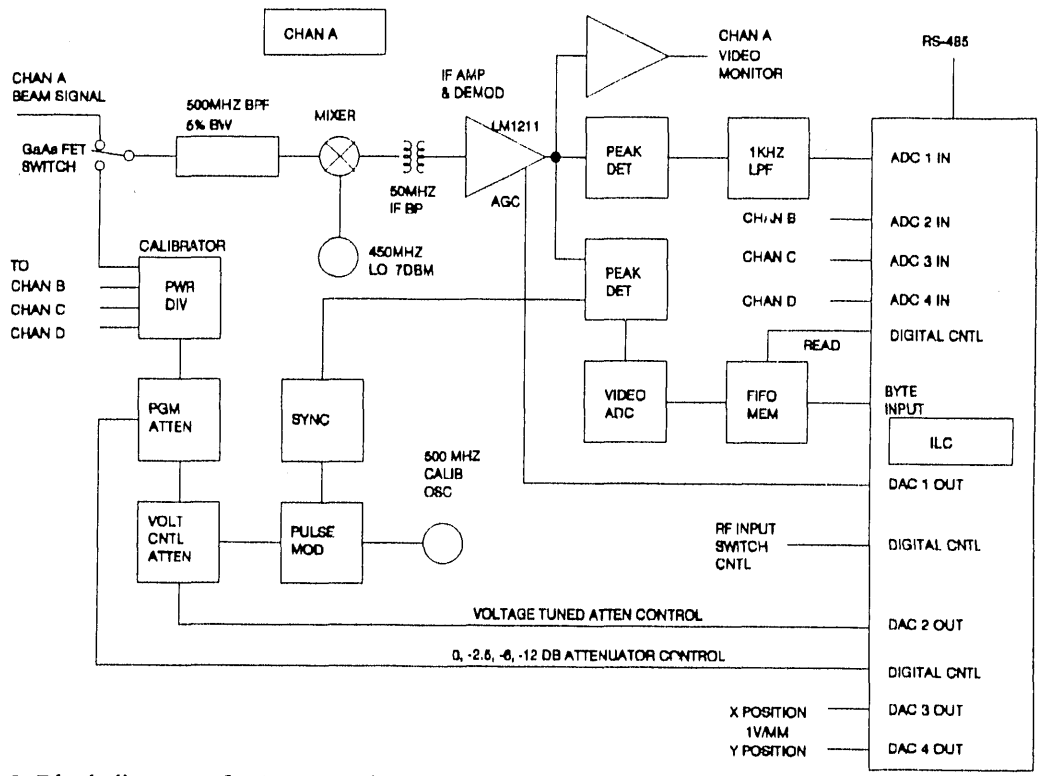


Fig. 8 Block diagram of a BPM receiver. One channel is shown.

RF Converter

The choice of operating frequencies for the RF converter was dictated by the requirement for arbitrary beam bunch-fill patterns in the storage ring. The two extremes of the fill patterns are a single high-current bunch or 328 bunches having equal charge. All patterns in between may exist though we expect the maximum number of bunches will be 250. A single 100 ps bunch rotating at $f_0$ (1.5 MHz) contains equal-amplitude harmonics of the rotation frequency to 2.5 GHz. With 328 bunches of equal charge and 30 ps duration, the beam harmonics begin at 500 MHz and extend beyond 10 GHz. We set the lower limit for the BPM operating frequency at 500 MHz because lower frequency beam rotation harmonics may be severely attenuated or disappear with certain fill patterns and because the pickups do not have good response below 200 MHz. Considering only

harmonics of the RF system and not those of the rotation frequency, we find the upper frequency limit for our BPM system is the beam channel cutoff frequency for waveguide mode propagation. In our case that frequency is about 4 GHz. We were left with eight frequencies from which to choose. We determined that cost essentially scales with frequency, so we chose 500 MHz as our operating frequency. Conventional wisdom dictates that one should not construct a sensitive instrument operating at the same frequency as nearby high-power RF systems. Two factors helped us in this regard. The beam channel will not propagate 500 MHz and the 100% shielding of the BPM signal cables will not admit 500 MHz interference. We have already determined how well these cables perform. The booster injection kicker magnet, a 50 MW, 100 ns pulsed system, does not affect nearby BPMs nor does the 40 KW, 500 MHz CW booster RF system. We believe the 300 kW storage ring RF system will have no impact on BPMs either.

The function of the RF converter module is to heterodyne 500 MHz beam signals down to 50 MHz and to inject calibration signals during the self-calibration sequence. There is no gain in this module. Figure 9 shows the basic circuitry. Standard IF components are available at 50, 60, and 70 MHz. We chose 50 MHz because we found an inexpensive 450 MHz surface-acoustic-wave (SAW) oscillator from RF Monolithics for the local oscillator.

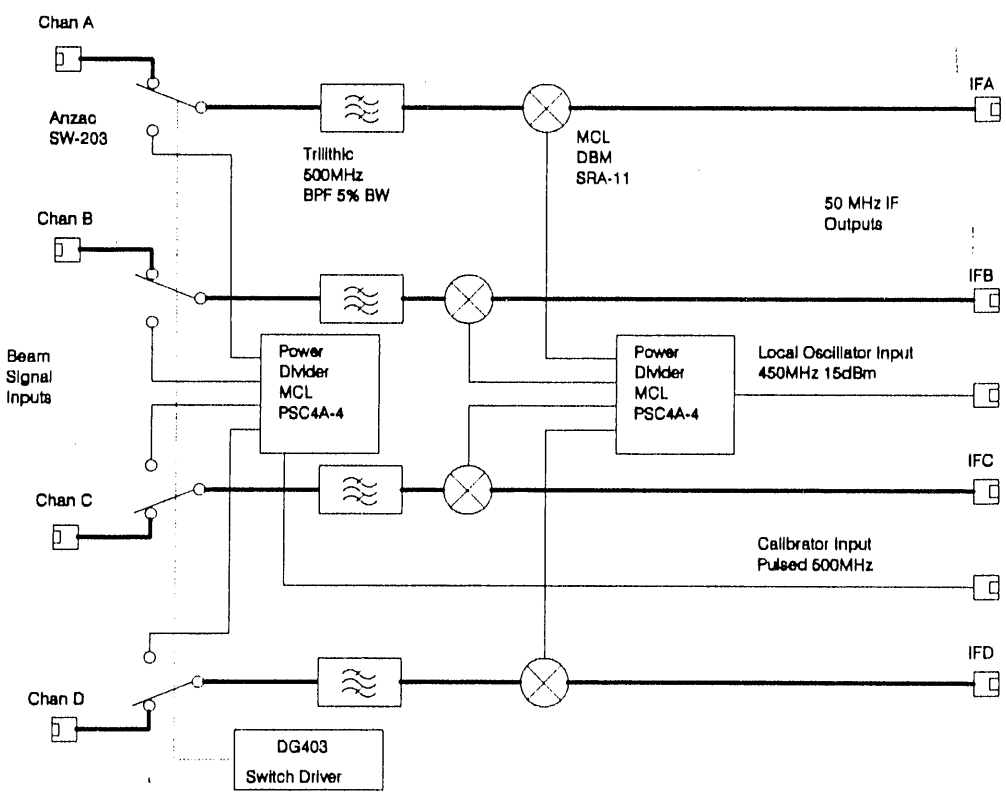


Fig. 9 RF Converter module. Darker lines indicate beam signal path.

We evaluated a number of circuit configurations for the RF converter in an effort to reduce the cost of this module. In our first prototype all components were connectorized. Isolation between channels was excellent and losses were low. Module assembly was difficult, and the unit was relatively expensive. We constructed an RF module having all components mounted on a PC board and interconnected with 50 ohm micro-strip line. Isolation between channels was only 30 dB

or so. Our specification for isolation was 60 dB. (We did not try a multi-layer board with shielded stripline.) After a few more iterations we had a hybrid module having only one connectorized component, the bandpass filter. All the other components are pin-connected to the PC board. Connections between components are made via short lengths of Belden 9307 coaxial cable. Isolation between channels is greater than 60 dB at our operating frequency.

The 500 MHz bandpass filter in the RF converter is an important component in the BPM. We tested a variety of filters for impulse response. SAW filters we tested had too much attenuation, long delay, and undesirable pulse feedthrough. Lumped LC filters soldered directly to the PC board exhibited pulse feedthough also (inadequate high-frequency isolation) and relatively high insertion loss. The best filters we found were tubular, 3-section, Chebychevs. They have excellent high frequency rejection and predicable pulse response. Better pulse response may be obtained with linear phase filters, but they are more costly. We found good agreement between SPICE evaluation of a 3-section, Chebychev bandpass filter at 500 MHz and a real filter. Figure 10 shows frequency and impulse response of the SPICE filter. The actual filter performs similarly.

The bandpass filter 3 dB-bandwidth is 25 MHz, much larger than required for single-turn position measurements in either the storage ring or booster. We could have tailored bandpass filter specifications to each application but determined it was less costly to customize the IF amplifiers. All of the RF modules are the same and will function in any of our applications.

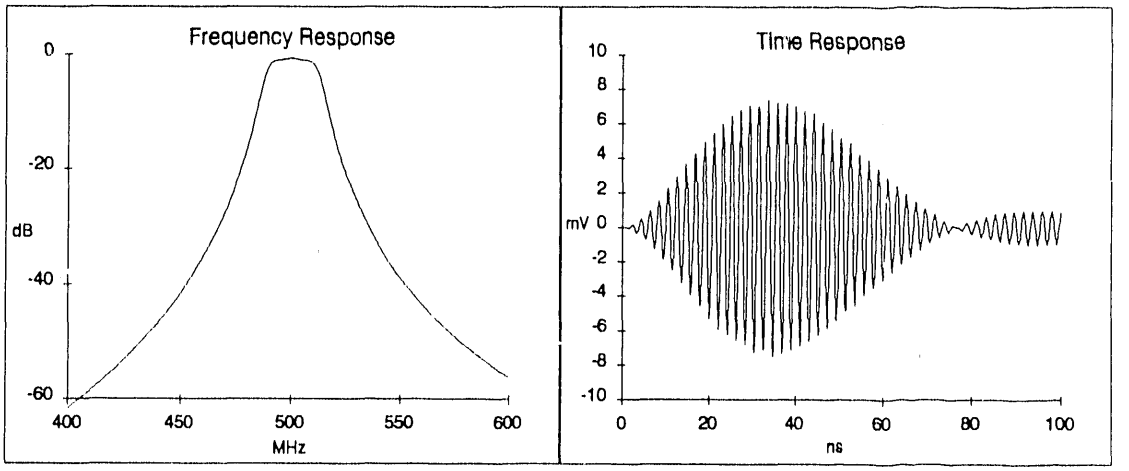


Fig. 10 RF module input bandpass filter response. Impulse - 100ps, 1V pulse.

IF Amplifier

A simplified schematic of the IF amplifier module appears in Figure 11. The RF module mixer output contains not only our 50 MHz beam signal, but many other mixer products. The IF module input filter passes the 50 MHz signals and terminates the out-of-band signals in 50 ohms. This particular IF bandpass filter from MCL makes mixer IF signal processing quite simple. The next component in the signal path is a MCL MAR-6 amplifier. This device has about 20 dB gain and a noise figure of less than 3 dB up to 1 GHz. This amplifier is optional in our design and so far, has not been required. Following the amplifier is a single-ended-to-differential transformer used to match 50Ω to the input impedance of the LM1211. This monolithic integrated circuit from National Semiconductor is a broadband demodulator system originally developed as a receiver for local area networks. It operates between 20 and 80 MHz and has over 40 dB IF gain-control range (AGC). The maximum gain of the IF amplifier section of the LM1211 is established by the input

resistors (Rin in figure 11) in the low-impedance common base input stage, the impedance of the IF tuned circuit, and the AGC current. The LM1211 (phase/amplitude) detector is driven by the signal appearing at the IF Out pin.

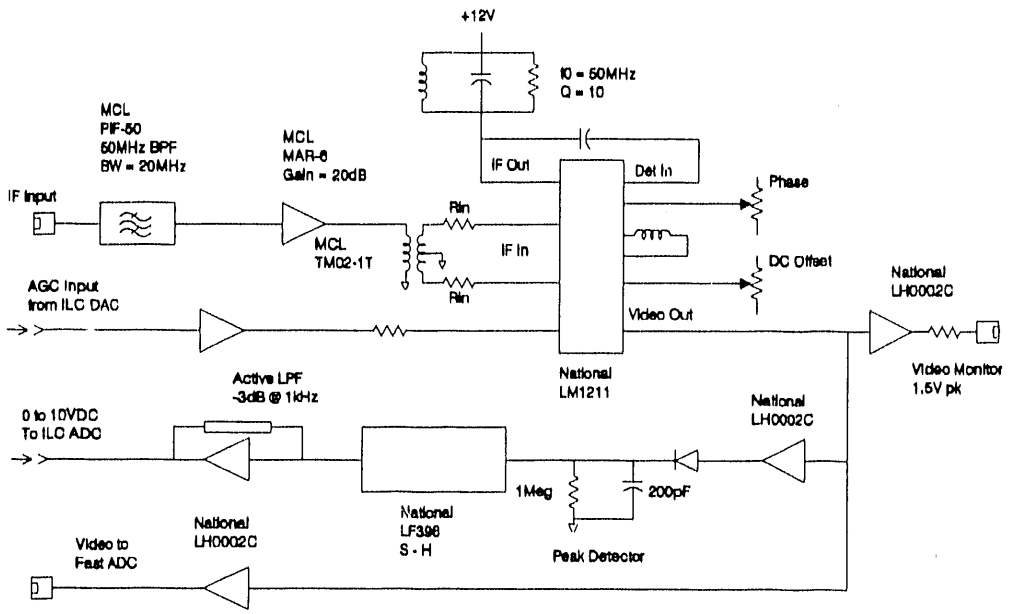


Fig. 11 Simplified schematic of IF amplifier module (1 of 4 in each bin).

The LM1211 detector operates with either AM or FM signals. For beam position monitoring we are interested in the amplitude of the 50 MHz IF signal, so we configured the detector as a quasi-synchronous, amplitude-modulation detector. By quasi-synchronous we mean that the internal phase detector is fed a reference signal developed from the IF signal itself. This of course means that no reference signal is available without an IF signal. A truly synchronous detector would have an unchanging reference signal of the proper frequency and correct phase. A limitation of quasi-synchronous detection is found when the internally-developed reference signal is no longer constant in phase and amplitude. This occurs when the IF signal is too low to saturate the output of the reference signal limiting amplifier. As a result we find a threshold below which the detector output is no longer useful. When this condition occurs, we increase the gain of the IF amplifier via AGC and restore good detector operation. At maximum gain the detector output is quite noisy, and much signal averaging is required in the ILC. At high signal levels we find some gain compression in the IF amplifier output and also some compression in the detector output as it approaches 3.5V.

The signal appearing at the Video Out pin on the LM1211 is a pulse, 0 to +3V, having the shape of the beam bunch pattern (within bandwidth limitations). A single beam bunch generates a waveform similar to Figure 10 (right) at the output of the RF module bandpass filter. After mixing and filtering, this burst of RF is amplified and detected by the LM1211. The detected pulse duration is determined by the bandwidth of the IF amplifier, and for a single bunch is about 150ns. When the beam bunch pattern contains many contiguous bunches, the tuned circuits reach steady-state performance and the pulse appearing at the Video Out pin has the general shape and duration of the beam bunch pattern.

The LM1211 has good carrier suppression at the video output so no additional filtering IF is required. The video output pulses are directed in three paths. A unity-gain buffer amplifier

delivers the pulses to a monitor jack on the rear of the BPM bin. The pulse amplitude is halved because of the amplifier's output impedance and cable impedance matching resistor. We use this pulse (and those from the other three IF amplifiers) for oscilloscope monitoring of BPM performance. Another buffer amplifier sends the pulse to a peak detector. When the BPM is monitoring low repetition rate beam (in the Linac for example) the sample-and-hold (S-H) circuit following the peak detector is used to capture the voltage peak. In this case the active low-pass filter following the S-H is simply used as a DC amplifier to scale voltages for the ILC ADC. When storage ring or booster beam is measured, the peak-detector output is essentially DC when the beam orbits continuously. In this case the S-H is used as an impedance buffer and simply tracks the input voltage. The low-pass filter following the S-H removes high frequency noise from the signal before it is digitized. The remaining path for the video output pulses is to a fast 8-bit digitizer which enables the BPM to make single-turn position measurements.

Tuning the IF amplifier and detector is simple. With a pulse modulated 50 MHz signal at the IF amplifier input, the Phase adjustment is set for best detected positive pulse response, and the DC offset is adjusted to remove DC voltage from the base of the pulse. A trim capacitor in the IF tuned circuit is adjusted for optimum pulse response also.

Fast Dual A/D Module (FAD)

There are two FAD modules in the storage ring and booster ring BPM bins. They are not used in the other locations. The function of these modules is to capture a time record of turn-by-turn beam position data for later analysis. A simplified block diagram of the FAD appears in figure 12. The video input of the FAD drives a fast peak detector having a MOS-FET reset switch. The peak detector output buffer amplifier drives the input of an 8-bit flash A/D. The A/D captures the voltage peak (2V maximum) and drives two first-in-first-out (FIFO) memory chips via an 8-bit buss.

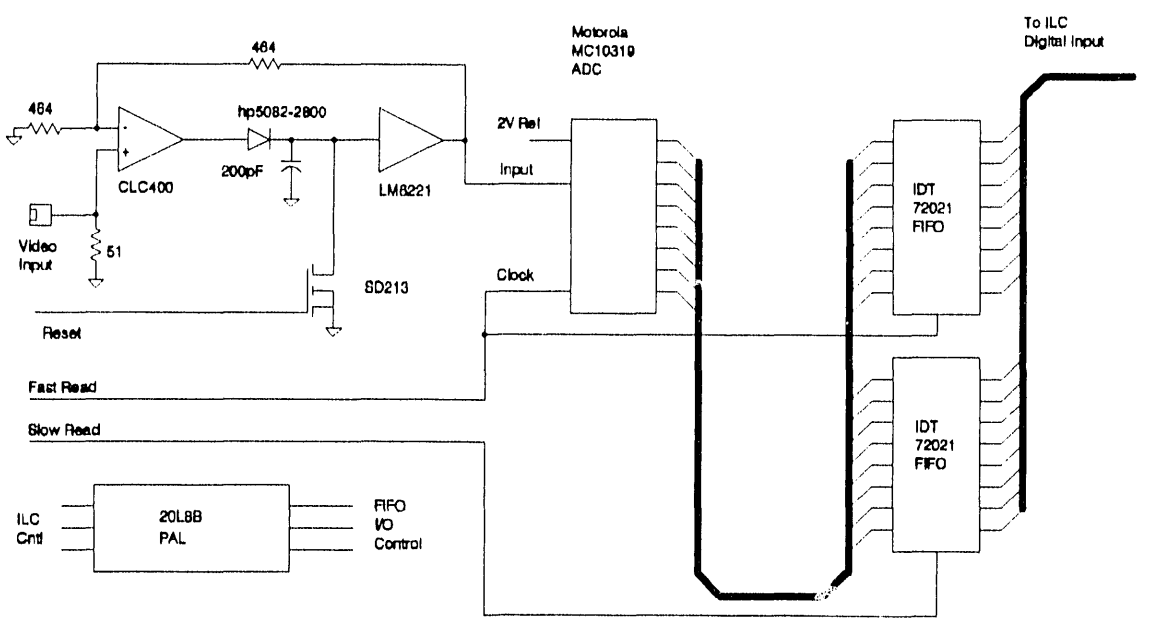


Figure 12. Simplified diagram of BPM Fast A/D module (one channel)

The timing of a FAD sequence is as follows: The ILC sets up FAD operation by clearing any old FIFO data and rearming trigger circuitry. Slightly before beam signals appear at the ring orbit frequency, the reset FET is gated on and the storage capacitor discharged. The FET drive pulse ends and the beam signal appears at the input of the peak detector. Just before the next ring orbit clock pulse arrives the A/D is triggered to acquire the peak of the detected beam signal. After A/D acquisition the FIFOs are strobed to store the data. One FIFO in each channel takes data at the ring orbit frequency. Another FIFO takes data at $f_0$, $f_0/10$, $f_0/100$, or $f_0/1000$, the rate being set in advance by the ILC via the Timing/Calibration module. This operation continues until an a-synchronous "Halt" pulse (derived in external circuitry) arrives at the bin promptly stopping signal acquisition. All BPM bins receive the "Halt" pulse at the same time. The ILC detects the halted condition and reads the contents of the FIFO memory. Input/output operation of the FIFOs is controlled by a programmable array logic (PAL) chip via commands from the ILC.

In the booster the BPM fast FIFO stores about 250 us of beam orbit data. The slow FIFO may have a time record 250 ms long (albeit with 999 out of 1000 beam signals missing). We are currently using the FAD data from booster BPMs to study beam injection performance. Code has been developed to quickly acquire and analyze the FAD data in the accelerator control system. Fast Fourier analysis of the booster X and Y position data reveals fractional tune. Analysis of data from all BPMs shows beam closed orbit.

Calibration/Timing Module

This module provides timing pulses for the IF and FAD modules. In addition, it generates calibration signals which are used to measure relative gain in the four channels. Input and output operations of the module are controlled by the ILC via a PAL chip. Figure 13 is a simplified electrical diagram of the module.

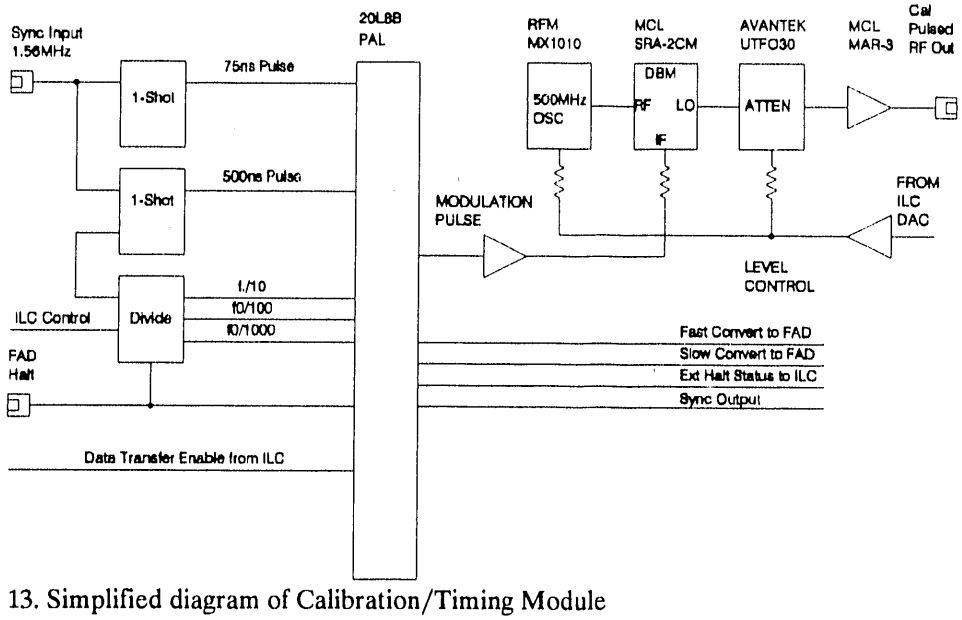


Figure 13. Simplified diagram of Calibration/Timing Module

The calibrator is used to measure differential gain in the RF, IF, and ILC modules. A calibration sequence goes as follows: After the gain of the IF amplifiers has been set by the ILC and beam signals have been acquired, the GaAs switches in the RF module are switched to the calibration input. The calibrator is off at this time as a sample of no-signal offsets is measured.

The beam signals are terminated in 50 ohms in the switches. Switch isolation at 500 MHz is about 50 dB. The calibrator is turned on, and the calibration signal level is automatically adjusted to equal the maximum detected beam signal. The difference between detected calibration signals is measured and gain-offset coefficients calculated. During subsequent beam measurements the measured offsets are subtracted from beam signals and gain coefficients applied to scale the raw beam signal data. With this method we have demonstrated 0.03 mm repeatability over a 40 dB range of RF test signals.

When the BPM measures multi-bunch beam the calibrator pulse length is set to 500 ns. Single bunch beam is simulated by a 75 ns calibration signal. This helps compensate slightly different transient response in the BPM amplifiers.

The calibration signal source is a SAW 500 MHz oscillator. This device has a modulation port which is useful in extending the calibration signal level control range. The RF output of the SAW oscillator drives the RF input of a doubly balanced mixer (DBM) used as an RF pulse modulator. A thin-film voltage-controlled attenuator (Avantek UTF-030) controls the level of the RF pulse at the input of the output buffer amplifier. The block diagram in Figure 8 shows another attenuator in the calibration signal path. This is a programmable step-attenuator used to precisely adjust the calibration signal level in 0.0, -2.5, -6.0, and -12.0 dB steps. When we wish to measure the relative linearity of the IF amplifiers and detectors, we use this attenuator during the calibration sequence to characterize the detectors at four distinct signal levels. This permits us to "linearize" the detectors[8]. Without this compensation, we see beam position errors develop as beam intensity falls. In some applications we may interrupt beam measurements to adjust the BPM gain and re-calibrate, restoring position accuracy. In situations where we may not interrupt the beam measurement for calibration, we rely on the detector linearization technique to give us the accuracy we require. Detector linearization provides about 10 dB dynamic range over which the beam intensity effects are about 0.03 mm.

Local Oscillator (LO)

The function of the LO is to provide the mixing signals required to heterodyne 500 MHz beam signals down to 50 MHz in the RF converter modules. The LO module is installed in the rear of the BPM bin in a small RF-tight enclosure. Figure 14 is a diagram of the this module.

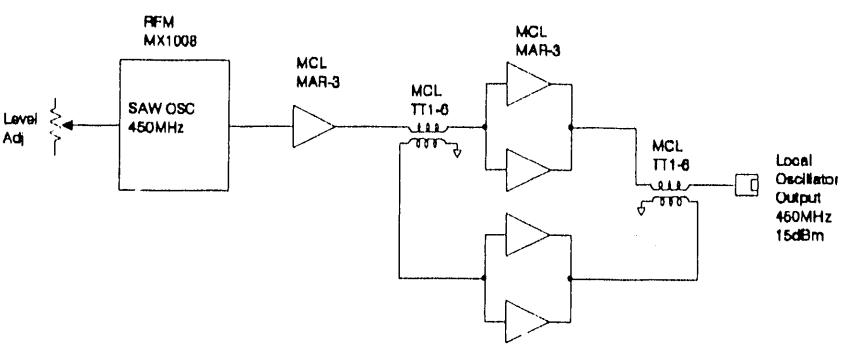


Figure 14. Simplified diagram of Local Oscillator module.

Early in the BPM design phase we considered synthesizing the LO signal from the accelerator master oscillator (500 MHz) and shipping it around the storage ring to all 96 BPM bins. We determined it was less costly to install an oscillator in each bin. Due to the wide bandwidth of the detectors, the LO frequency stability requirements are not severe. The SAW oscillators we are using (from RF Monolithics) are accurate within 100 kHz and their phase noise

is acceptably low. (RFM refers to these oscillators as UHF Microtransmitters.) The SAW oscillator power output is adjustable over a 50 dB range up to a maximum of about +10 dBm via an amplitude-modulation port. In the LO we use this port to set the output level for best spectral performance (lowest distortion). We added amplifiers (MCL MAR-3) to boost the LO output to +15 dBm. A hybrid power-splitter in the RF Converter module reduces the LO power to +7 dBm as required by the RF module mixers.

Intelligent Local Controller (ILC)

This module is at the lowest level of the ALS computer control system[9]. Throughout the ALS nearly 600 ILCs will be used to control commercial instruments via RS-232 or the GPIB, run and monitor magnet power supplies, control beam-line components, and run the major systems such as high-power RF amplifiers. BPMs now use 50 ILCs, and 100 more are under construction.

The ILC is the functional equivalent of a Multibus-I or a VME chassis except that it controls fewer devices. It is smaller than these other controllers, fitting in a 3U Eurocard module, and consumes only 5 W. The ILC has three processors; an 80C186, a companion floating-point math coprocessor, and an intelligent serial link controller. These chips share 64 kbytes of dual-ported, battery-backed memory. ILC input/output consists of four channels of 13 bit ADC, four channels of 16 bit DAC, 24 bits of digital I/O, and a 2 Mbit/s serial link to other ILCs and the upper echelon of the accelerator control system. Most of the ILC digital I/O may be configured for either input or output. Additional I/O capability is available with the installation of special daughter-cards connected to an SBX port on the ILC. Through the SBX connector and appropriate cards, we control GPIB devices, RS-232 instruments, or expand the digital I/O by 24 bits. An improved version of the ILC is in the design phase. We expect a 60% increase in speed, four times the memory, 16 bit ADCs, and even less power consumption. Figure 15 is a block diagram of the current ILC architecture.

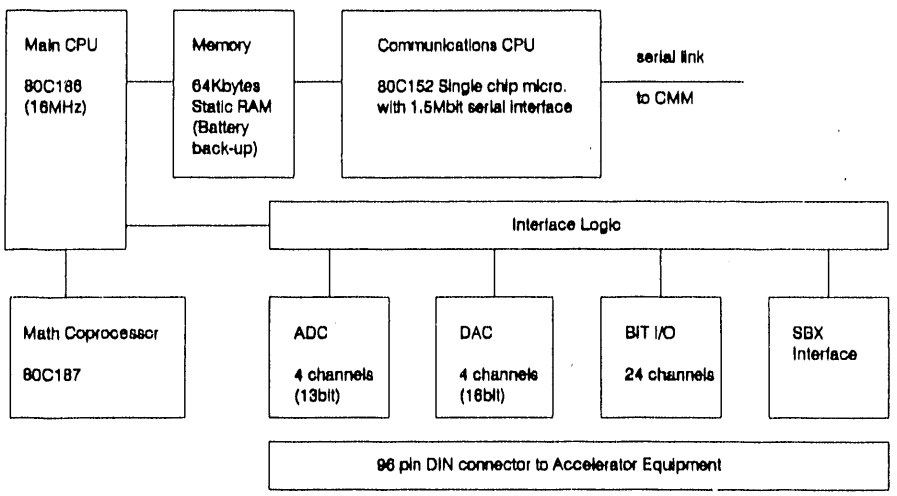


Figure 15. ILC module architecture.

The ALS instrumentation staff developed code for the BPM ILCs in a PC environment using Microsoft Quick Basic 4.5. Programming of the ILC for operation in the accelerator systems is done in C or PLM languages, generally by the Control System staff. In order for us to develop our BPM code we were supplied with Quick Basic libraries, an ILC data base having unique names for

each BPM ILC I/O function, and the necessary hardware for PC to ILC communications. We developed a considerable amount of code for testing and developing BPM hardware. Our Basic code ran in the PC, so we did not achieve maximum performance from the ILC. As our code matured, certain functions were programmed into the ILC improving position calculation speed dramatically. In the end we were able to get 30 readings of X and Y position per second with each reading averaged 50 times. Speed is not an issue in the ALS injector BPMs because of the low beam repetition rate. In the storage ring we expect we will achieve about 50 Hz performance with each reading averaged 50 times. Our plan is to synchronize readings in all 96 storage ring BPMs at variable rates set by the machine operator. Total bandwidth for 96 BPM readings and subsequent beam orbit correction will be at least 10Hz and probably higher.

When FAD data are collected and processed by the ILC we see FFTs of X and Y position from a single booster BPM displayed in the control room in a few seconds. Collecting data from all 32 BPMs and displaying data takes a few seconds longer. We are currently working on a real time (1 Hz) display of fractional betatron tune using data from booster BPM FADs. Closed orbit displays will be displayed at 1 Hz also.

Power Supply

Two open-frame linear power supplies are installed in the rear of the BPM bins. We decided not to use smaller switcher power supplies because of the RF noise they generate. The power supplies provide +15, -15, +5, and -5.2 V at about 80 W.

## Error Correction

Figures 16 - 18 show how our single-point calibration and multi-point linearization routines improve the BPM performance. The signal source for these tests was a CW generator at 50 MHz connected to the inputs of four IF modules. The the RF input voltage was stepped in 1 mV increments up to 100 mV. Three 180 degree hybrid power dividers evenly split the signal between modules. The gain of the IF modules was set to give full scale voltage at 100 mV into the hybrids. Figure 16 shows the raw DC voltage out of the IF Amplifier/Detector modules and the calculated X and Y positions. The position errors are rather large due to gain differences in the IF modules. Figure 17 shows the effect of a single point calibration at 70 mV input. Notice the detector gains are equal at 70 mV and the X and Y beam position is zero as it should be for equal inputs. Notice also that the calculated position deviates greater that 0.03 mm as the voltage is changed less than a factor of two. Below 10 mV input the calculated position error is large due to the LM1211 detector threshold. Figure 18 shows how the linearization technique overlays the raw data. A straight line is included in the graph for comparison. The position plot for linearized data shows good performance to about 10 dB below full scale.

I stated that we have a method for correcting the pin-cushion distortion we observe in the storage ring BPM response. In order to use this method we must make linear measurements of the button voltage. In our tests of the correction method we used a wire and a network analyzer to measure button response to wire motion. A 20 mm displacement in a single axis resulted in button voltages differing by a factor of 10 or so. When the wire was placed at 20 mm in X and Y, the button nearest the wire developed voltages nearly 100 times higher than the opposing button. To accurately measure voltages over such a dynamic range a very good detector (one essentially as linear as the network analyzer detector) is required. With all of our error correction schemes the LM1211 detector will never be that good.

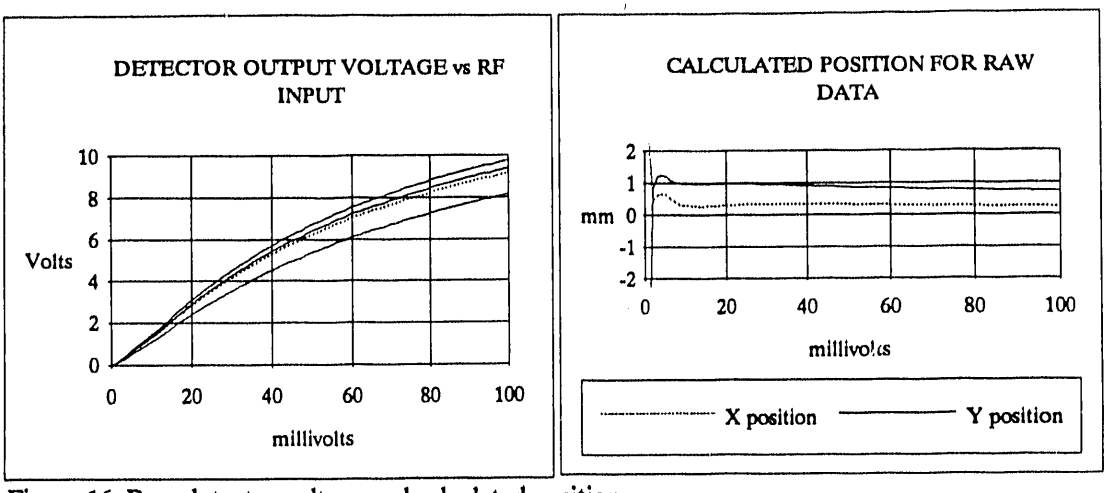


Figure 16. Raw detector voltage and calculated position.

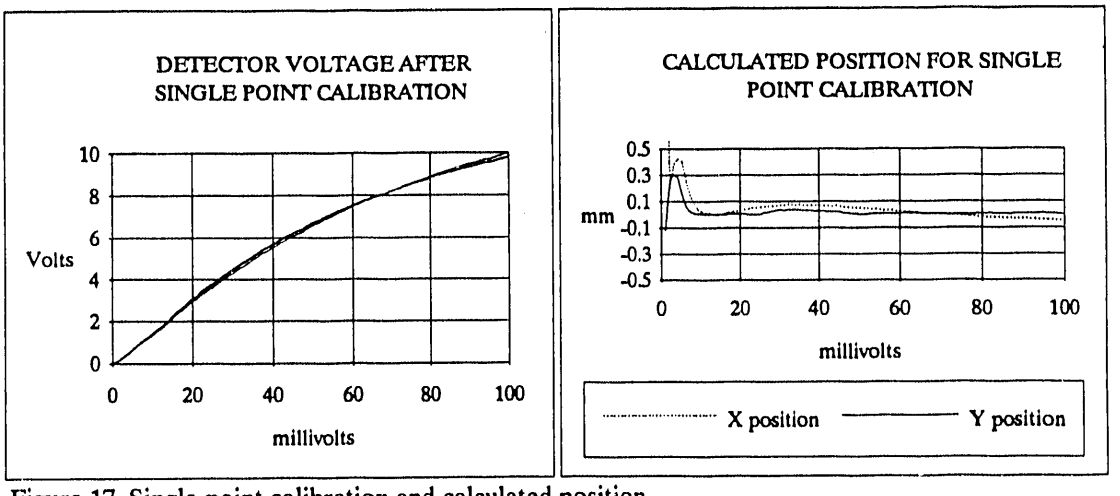


Figure 17. Single point calibration and calculated position.

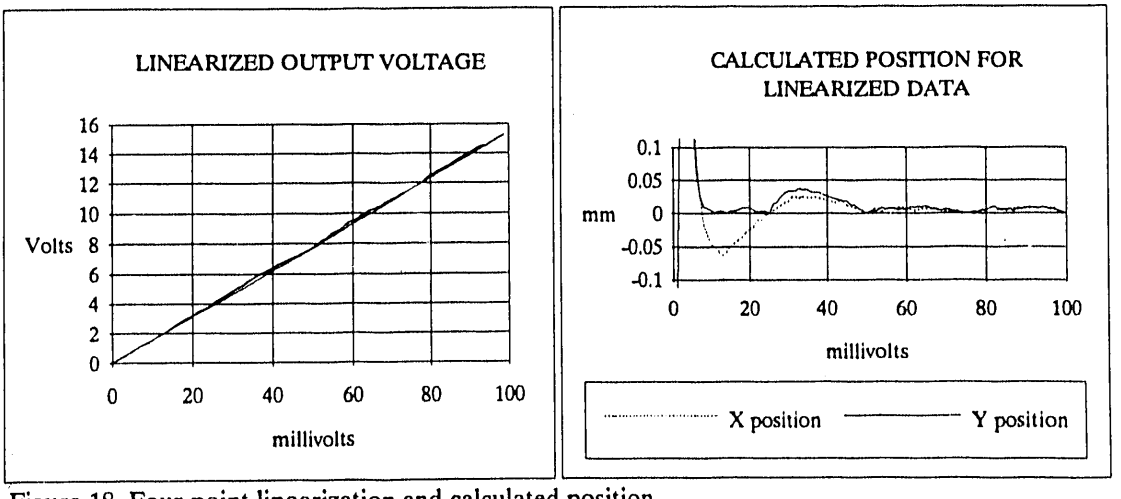


Figure 18. Four point linearization and calculated position.

The ALS storage ring beam is not expected to be off center by more than a few millimeters in normal operation. The vertical aperture will ultimately be limited to 10mm by insertion devices. We expect we will be able to correct for pin-cushion distortion over the anticipated range of beam motion. One may argue that accurate measurements of beam position well off the beam pipe center are not required, that is, we must know only what direction to steer the beam to get it back on center. That may be true, but prudence dictates we should have a method for accurate measurements when the beam orbit is less than perfect.

## Conclusion

I have described the ALS beam position monitor and how it is working as we commission the beam injection systems. Having single-turn measurement capability has made the booster BPMs very useful at this early stage. We expect this feature will helpful in commissioning the storage ring also.

The wide bandwidth we require for single-turn measurements made error correction a major task in the BPM development. A single receiver/detector BPM multiplexed to four pickups would certainly have fewer systematic offsets and gain errors requiring compensation. Indeed, we plan to install such systems for beam position monitoring at the entrance and exit of insertion devices. These BPMs (modeled after the NSLS X-ray ring BPMs[10]) will be used for the most accurate and stable monitoring in the storage ring. They will also be part of the active interlock system we will use to prevent vacuum chamber damage due to mis-steered photon beam.

## Acknowledgements

My thanks go to a number of people for helping in the development of the BPM. Jim Johnston did much of the circuit design, lab work, and software development. Mike Fahmie coded the PALs. Steve Magyary provided the ILCs and translated BASIC code to PLM. Chris Timossi built and coded the ILC BPM data base. Al Geyer is currently building 100 more BPM bins. I am particularly thankful for an interactive and productive relationship with Tom Henderson, John Meneghetti, and Kurt Kennedy of the ALS Mechanical Engineering staff while we designed the BPM pickups.

## References


[1] J. Hinkson, J. Johnston, I. Ko, "Advanced Light Source (ALS) Beam Position Monitor," in Proceedings of the IEEE Particle Accelerator Conference, Vol. 3, p. 1507. (1989)

[2] R. Shafer, "Beam Position Monitoring," AIP Conference Proceedings, 212, E Beadle & V Castillo Ed., p 26, (1989)

[3] R. Littauer, "Beam Instrumentation," AIP Conference Proceedings, 105, M. Month, Ed., p. 869, (1983)

[4] K. Halbach, "Description of Beam Position Monitor Signals with Harmonic Functions and their Taylor Series Expansions," Lawrence Berkeley Laboratory AFRD Report, LBL22840

[5] G. Lambertson, "Calibration of Position Electrodes Using External Measurements," Lawrence Berkeley Laboratory Advanced Light Source Internal Note LSAP05, (1987)

[6] G. Decker, Y. Chung, E. Kahana, "Progress on the Development of APS Beam Position Monitoring System," Presented at IEEE PAC, San Francisco (1991)

[7] J. Borer, et al., "The LEP Beam Orbit Measurement System," in Proceedings of the IEEE Particle Accelerator Conference, Vol, 2, p. 778, (1987)

[8] J. Hinkson, Jim Johnston, H. Lancaster, "Linearizing the Electronics of the ALS Beam Position Monitor," LBL Advanced Light Source Internal Note LSEE061, (1989)

[9] S. Magyary, et al., "Advanced Light Source Control System," in Proceedings of IEEE Particle Accelerator Conference, Vol. 1, p. 74, (1989)

[10] R. Biscardi, J. Bittner, "Switched Detector for Beam Position Monitor," in Proceedings of IEEE Particle Accelerator Conference, Vol 3. p. 1516, (1989)



This work was supported by the Director, Office of Energy Research, Office of Basic Energy Sciences, Materials Sciences Division of the U.S. Department of Energy, under Contract No. DE-AC03-76SF00098.

# END

DATE
FILMED
5108192